
Linear and Nonlinear Analysis
Yokohama Publishers
ISSN 2188-8167

Volume 10, Number 1, 2024, 35–44

THE FOURTH-ORDER NONLINEAR EVOLUTION EQUATION FOR APPLICATION TO DEEP WATER CAPILLARY-GRAVITY WAVES INCLUDING THE EFFECT OF WIND FLOW

SOURAV HALDER AND A. K. DHAR

Abstract. A fourth-order nonlinear evolution equation (NLEE) for the propagation of three-dimensional capillary-gravity waves (CGW) on deep water in the presence of current jump is derived using multi-scale expansion. From this equation we have made the stability analysis of a plane progressive wave. We have presented here the analytical results for long wavelength sideband instability of small amplitude waves (Stokes waves). The expressions for growth rate of instability (GRI) for both one-dimensional and two-dimensional perturbations and maximum GRI are obtained from the nonlinear dispersion relation. It is to be noted that fourth-order results considerably modify the sideband instability behaviors of weakly nonlinear waves. It is observed from figures that the maximum GRI obtained from fourth-order result enhances with the enhancement of wave steepness and then it decreases, while maximum GRI obtained from third-order result enhances steadily with the increase of wave steepness. Maximum GRI is found to decrease with the increase of wind velocity. Further, the maximum GRI first increases slightly up to certain value of wave steepness and then it decreases due to the effect of capillarity. From the contour plots, it is seen that the region of instability reduces with the increase of wind velocity, whereas it increases with the increase of both the wave steepness and surface tension.

1. Introduction

In the analysis of nonlinear evolution of surface water waves, nonlinear Schr 日 dinger equation (NLSE) are generally applied as it can appropriately reflect the sideband instability. This analysis is adequate for small wave amplitude and for long wavelength perturbations. For wave amplitude larger than 0.15 predictions from the NLSE do not comply with the exact numerical results of Longuet-Higgins [9], [10]. Dysthe [2] first pointed out that the stability analysis starting from fourth-order nonlinear evolution equation (NLEE) provides results compatible with the results of Longuet-Higgins [9], [10] for wave amplitude up to 0.25. So it can be stated that the fourth-order NLEE is an excellent starting point for analysing sytability properties of water waves in deep water. From fourth-order NLEE Janssen [8] has developed on the Dysthe's approach by studying the influence of wave induced mean flow on the long time nature of sideband instability. Derivations of fourth-order NLEE for

2020 *Mathematics Subject Classification.* 76B07, 76B15, 76B45.

Key words and phrases. Nonlinear evolution equation, Capillary-gravity waves, Wind velocity, Sideband instability.

infinite depth of water by considering several effects were performed by different authors such as Stiassnie [12], Hogan [4], Dhar and Das [3].

It is to be noted that the gravity-capillary waves (CGW), which in general are generated due to wind flow and form a shear current in the topmost water layer. Brantenberg and Brevik [1] have used a cubic-order Stokes expansion for CGW travelling on an opposing current and later on, Hsu et al. [5] have elaborated that works and obtained the third-order solution of CGW travelling on finite depth water surface in the presence of constant vorticity. Hur [6] investigated the sideband instability for CGW including the effect of vorticity. Hsu et al. [7] have also derived a third-order NLSE for CGW in the presence of constant vorticity. They have reported that the combined effect of vorticity and capillarity is to enhance the growth rate of instability (GRI) influenced by surface tension when vorticity is negative.

In the present paper we have presented the stability analysis of a uniform wave-train travelling at the interface of two fluids of infinite depths including the effect of wind flow using fourth-order NLEE derived by Majumder and Dhar [11]. The paper is organized as follows: the framework for the problem is formulated in section 1, the fourth-order NLEE is given in section 2, section 3 deals with stability analysis and some important results, and finally conclusion is given in section 4.

2. NLEE for interfacial waves

We begin with the following fourth-order NLEE, which has been derived by Majumder and Dhar [11] in the case of air flowing over water. This paper was to obtain the influence of wind blowing over water on Benjamin-Feir instability (BFI)

$$\begin{aligned} 2i\frac{\partial\alpha}{\partial\tau} - \delta_1\frac{\partial^2\alpha}{\partial\xi^2} + \delta_2\frac{\partial^2\alpha}{\partial\eta^2} + i\delta_3\frac{\partial^3\alpha}{\partial\xi^3} + i\delta_4\frac{\partial^3\alpha}{\partial\xi\partial\eta^2} &= \Lambda_1\alpha^2\alpha^* + i\Lambda_2|\alpha|^2\frac{\partial\alpha}{\partial\xi} \\ &\quad + i\Lambda_3\alpha^2\frac{\partial\alpha^*}{\partial\xi} + \Lambda_4\alpha\mathcal{H}\frac{\partial}{\partial\xi}(|\alpha|^2), \end{aligned} \tag{2.1}$$

where $\xi = x_1 - c_g t_1$, $\eta = y_1$, $\tau = \epsilon t_1$, the coefficients δ_i, Λ_i, $(i = 1, 2, 3, 4)$ are given in Appendix and $\mathcal{H}$ is the Hilbert transform operator defined by

$$\mathcal{H}(\Phi) = \frac{1}{2\pi}\int\int_{-\infty}^{\infty}\frac{(\xi^{'} - \xi)\Phi(\xi^{'}, \eta^{'})}{[(\xi^{'} - \xi)^2 + (\eta^{'} - \eta)^2]^{3/2}}d\xi^{'}d\eta^{'}$$

Herein, the group velocity c_g of the carrier wave given by

$$c_g = \frac{2\gamma v(\sigma - v) + (1 - \gamma) + 3\kappa}{2[\sigma + \gamma(\sigma - v)]},$$

where v denotes the uniform velocity of wind flowing parallel to x axis, γ is the density ratio of air to water and $\kappa = \frac{Tk^2}{\rho g}$ is non-dimensional surface tension coefficient. The carrier frequencies of two modes of wave propagation are $\sigma_\pm = \{\gamma v \pm \sqrt{1 - \gamma^2 - \gamma v^2 + (1 + \gamma)\kappa}\}/(1 + \gamma)$.

For linear stability $|v| \leq \sqrt{\{1-\gamma^2+(1+\gamma)\kappa\}/\gamma}$, so our analysis will continue to be valid if the wind velocity v is less than critical velocity, $v_c = \sqrt{\{1-\gamma^2+(1+\gamma)\kappa\}/\gamma}$. For air-water interface $\gamma = 0.00129$ and for $\kappa = 0$ this critical value becomes 27.8423.

If we set $\kappa = 0$, then the evolution equation (2.1) reduces to an equation equivalent to equation (34) of Dhar and Das [3].

3. Stability analysis for finite amplitude wavrtrain

The solution of equation (2.1) is given by

$$\alpha = \frac{\eta_0}{2}\exp\left(\frac{-i\Lambda_1}{8}\eta_0^2\tau\right), \tag{3.1}$$

where η_0 is called the wave steepness.

Now we consider the perturbation in the uniform solution given by

$$\alpha = \frac{\eta_0}{2}(1+\eta^{'})\exp\left[i\left(\theta^{'}-\frac{\Lambda_1}{8}\eta_0^2\tau\right)\right], \tag{3.2}$$

in which $\eta^{'}$, $\theta^{'}$ are small real perturbations of amplitude and phase respectively and their time dependence is of the form $\exp(-i\Omega^{'}\tau)$.

Inserting (3.2) in (2.1) and linearizing we get two equations for $\eta^{'}$ and $\theta^{'}$. Next taking the Fourier transform of two linear equations with respect to ξ, η, we get the following two algebraic equations (3.4) and (3.5) for the two quantities $\overline{\eta^{'}}$ and $\overline{\theta^{'}}$, which are the Fourier transforms of $\eta^{'}$ and $\theta^{'}$ respectively, given by

$$(\overline{\eta^{'}},\overline{\theta^{'}}) = \frac{1}{2\pi}\int\int_{-\infty}^{\infty}[\eta^{'}(\xi,\eta),\theta^{'}(\xi,\eta)]e^{-i(\lambda\xi+\mu\eta)}\,d\xi d\eta \tag{3.3}$$

$$\left[\overline{S}_1+\frac{(\Lambda_2+\Lambda_3)}{8}\eta_0^2\lambda\right]\overline{\eta^{'}}+i\overline{S}_2\overline{\theta^{'}}=0 \tag{3.4}$$

$$\left[\overline{S}_1+\frac{(\Lambda_2-\Lambda_3)}{8}\eta_0^2\lambda\right]\overline{\theta^{'}}-i\left[\overline{S}_2-\frac{\Lambda_1}{4}\eta_0^2\left(1-\frac{\Lambda_4\lambda^2}{\Lambda_1\sqrt{\lambda^2+\mu^2}}\right)\right]\overline{\eta^{'}}=0, \tag{3.5}$$

where $\overline{S}_1 = \Omega - c_g\lambda + \frac{1}{2}(\delta_3\lambda^3+\delta_4\lambda\mu^2)$, $\overline{S}_2 = \frac{1}{2}(\delta_1\lambda^2-\delta_2\mu^2)$, and $\Omega = \Omega^{'}+c_g\lambda$.

From equations (3.4) and (3.5) we obtain the nonlinear dispersion relation as follows

$$\left[\overline{S}_1+\frac{(\Lambda_2+\Lambda_3)}{8}\eta_0^2\lambda\right]\left[\overline{S}_1+\frac{(\Lambda_2-\Lambda_3)}{8}\eta_0^2\lambda\right] = \overline{S}_2\left[\overline{S}_2-\frac{\Lambda_1}{4}\eta_0^2\left(1-\frac{\Lambda_4\lambda^2}{\Lambda_1\sqrt{\lambda^2+\mu^2}}\right)\right] \tag{3.6}$$

Solving for $\overline{S}_1$, we have

$$\overline{S}_1 = -\frac{\Lambda_2}{8}\eta_0^2\lambda \pm \sqrt{\overline{S}_2\left[\overline{S}_2 - \frac{\Lambda_1}{4}\eta_0^2\left(1 - \frac{\Lambda_4\lambda^2}{\Lambda_1\sqrt{\lambda^2+\mu^2}}\right)\right] + \frac{\Lambda_3^2}{64}\eta_0^4\lambda^2} \tag{3.7}$$

From this relation we obtain the following expression for perturbed frequency

$$\begin{aligned}\Omega = c_g\lambda - \frac{\delta_3}{2}\lambda^3 - \frac{\delta_4}{2}\lambda\mu^2 - \frac{\Lambda_2}{8}\eta_0^2\lambda \\ \pm\frac{1}{2}\sqrt{(\delta_1\lambda^2 - \delta_2\mu^2)\left[\delta_1\lambda^2 - \delta_2\mu^2 - \frac{\Lambda_1}{2}\eta_0^2\left(1 - \frac{\Lambda_4\lambda^2}{\Lambda_1\sqrt{\lambda^2+\mu^2}}\right)\right] + \frac{\Lambda_3^2}{16}\eta_0^4\lambda^2}\end{aligned} \tag{3.8}$$

For instability we have

$$(\delta_1\lambda^2 - \delta_2\mu^2)\left[\delta_1\lambda^2 - \delta_2\mu^2 - \frac{\Lambda_1}{2}\eta_0^2 + \frac{\Lambda_4\eta_0^2\lambda^2}{2\sqrt{\lambda^2+\mu^2}}\right] + \frac{\Lambda_3^2}{16}\eta_0^4\lambda^2 < 0 \tag{3.9}$$

The first two terms in both the first and also in the second factors in (3.9) come from the third-order dispersive terms which are second and third terms of the left side of (2.1). In the second factor of (3.9) the third and fourth terms come respectively from the third-order and the fourth-order nonlinear terms, which are respectively the first and fourth terms of the right side of (2.1). Also, the last term in (3.9) comes from the fourth-order nonlinear term, which is the third term of the right side of (2.1). Here, we observe that the higher-order dispersive terms of (2.1) do not contribute to the stability character, whereas the higher-order nonlinear term involving Hilbert's transform influence significantly the stability character.

If condition (3.9) is fulfilled, the perturbed frequency Ω will be complex-valued and the GRI represented by the imaginary part Ω_i of Ω becomes

$$\Omega_i = \sqrt{(\delta_1\lambda^2 - \delta_2\mu^2)\left[\frac{\Lambda_1}{2}\eta_0^2 - \delta_1\lambda^2 + \delta_2\mu^2 - \frac{\Lambda_4\eta_0^2\lambda^2}{2\sqrt{\lambda^2+\mu^2}}\right] - \frac{\Lambda_3^2}{16}\eta_0^4\lambda^2} \tag{3.10}$$

For one-dimensional perturbation $\mu = 0$, so that (3.9) and (3.10) take the forms

$$\delta_1\left[\delta_1\lambda^2 - \frac{\Lambda_1}{2}\eta_0^2 + \frac{\Lambda_4\eta_0^2|\lambda|}{2}\right] + \frac{\Lambda_3^2}{16}\eta_0^4 < 0 \tag{3.11}$$

$$\Omega_i = \lambda\sqrt{\delta_1\left[\frac{\Lambda_1}{2}\eta_0^2 - \delta_1\lambda^2 - \frac{\Lambda_4\eta_0^2|\lambda|}{2}\right] - \frac{\Lambda_3^2}{16}\eta_0^4} \tag{3.12}$$

Omitting fourth-order terms of (3.12) one can find

$$\frac{\Omega_i}{\eta_0^2} = \frac{\lambda}{\eta_0}\sqrt{\frac{\delta_1\Lambda_1}{2} - \delta_1^2\left(\frac{\lambda}{\eta_0}\right)^2} \tag{3.13}$$

The expression for maximum GRI is given by

$$G_m = \frac{\Lambda_1}{4}\left[1 - \frac{\Lambda_4\eta_0}{2\sqrt{\Lambda_1\delta_1}}\right]\eta_0^2 \tag{3.14}$$

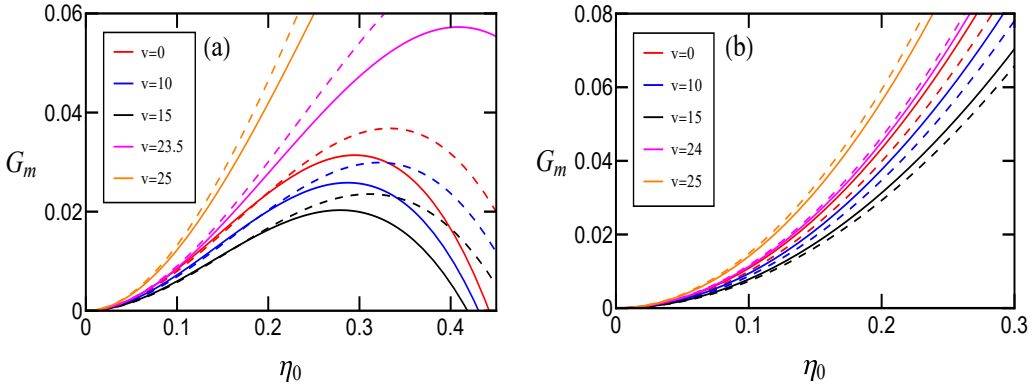

FIGURE 1. Plot of G_m versus η_0 for $\gamma = 0.00129$ and different values of v and κ ; : $\kappa = 0$, : $\kappa = 0.035$; (a) fourth-order result, (b) third-order result.

which occurs for the wavenumber

$$\lambda_m = \frac{1}{2}\left[\sqrt{\frac{\Lambda_1}{\delta_1}} - \frac{3\Lambda_4}{8\delta_1}\eta_0\right]\eta_0 \tag{3.15}$$

At marginal stability $\Omega_i = 0$, then the perturbed frequency takes the form

$$\Omega_r = c_g\lambda = c_g\left[\sqrt{\frac{\Lambda_1}{2\delta_1}} - \frac{\Lambda_4}{4\delta_1}\eta_0\right]\eta_0 \tag{3.16}$$

and the value of Ω_{rm} corresponding to λ_m is

$$\Omega_{rm} = c_g\lambda_m = \frac{c_g}{2}\left[\sqrt{\frac{\Lambda_1}{\delta_1}} - \frac{3\Lambda_4}{8\delta_1}\eta_0\right]\eta_0 \tag{3.17}$$

The maximum GRI, G_m has been drawn in Fig. 1 as a function of wave steepness η_0 for several values of v and κ. It is seen that G_m obtained from fourth-order result first increases with η_0 and then decreases, while G_m computed from third-order result increases steadily with η_0. The most important finding is that the maximum GRI decreases with the increase of wind velocity. Also the maximum GRI is found to be appreciably much higher for wind velocity approaching its critical value. Further, the maximum GRI first increases slightly up to certain value of wave steepness and then it decreases due to the effect of capillarity.

The perturbed frequency Ω_r at marginal stability and contour plots of frequency separation of fastest growing sideband Ω_{rm} have been plotted in Fig. 2 and Fig. 3 respectively against η_0 for different values of v and κ. The effects of wind velocity and surface tension are captured in both the figures.

Fig. 4 shows that the GRI, Ω_i/η_0^2 as a function of λ/η_0 for $\gamma = 0.00129$ and different values of v and κ. It is shown that Ω_i/η_0^2 increases with the increase of

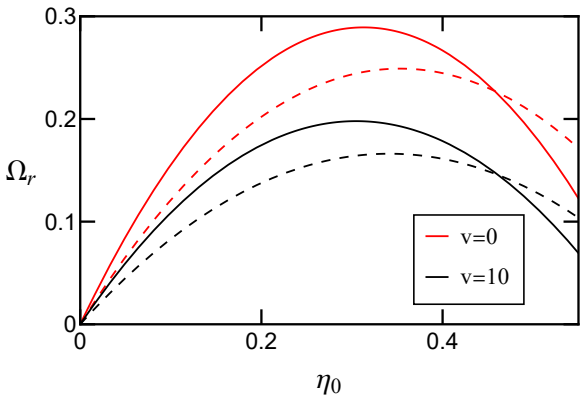

FIGURE 2. Curves of marginal stability versus η_0 for $\gamma = 0.00129$ and different values of v and κ; $\backslash\kappa = 0\backslash\kappa = 0.035$.

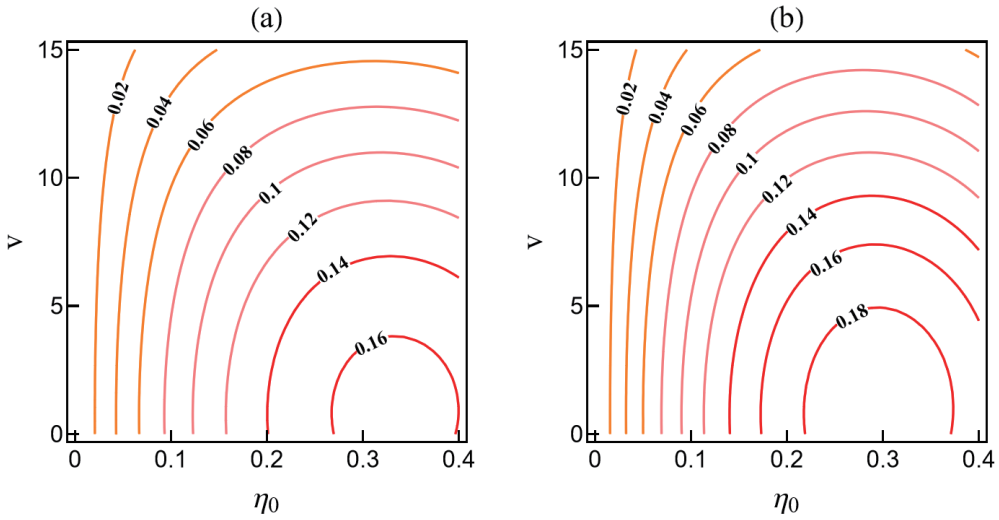

FIGURE 3. Contour plots of frequency separation of fastest growing sideband $\Omega_{rm}(\eta_0, v)$ for $\gamma = 0.00129$; (a) $\kappa = 0$, (b) $\kappa = 0.035$.

wind velocity up to certain critical value of λ/η_0 and then it diminishes. Also GRI is observed to be considerably higher for wind velocity approaching its critical value.

In Figs. 5 and 6 we have shown some contour plots of GRI, Ω_i in perturbed wavenumber plane ($\lambda\mu$- plane) for $\gamma = 0.00129$ and several values of v, κ and η_0. We have noticed some change in the shape and span of the contours along both the axes. It is found that the instability region reduces with the increase of wind velocity, whereas it increases with the increase of both η_0 and κ.

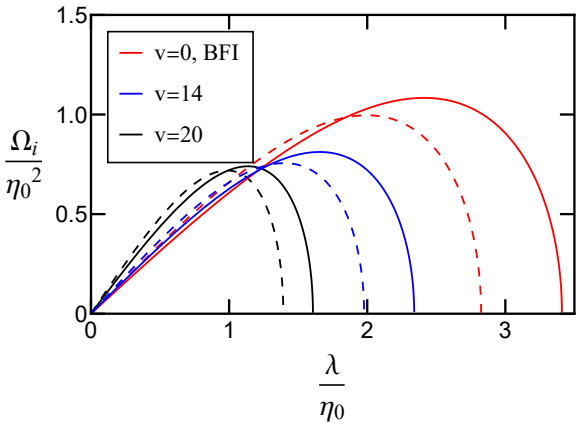

FIGURE 4. Plot of Ω_i/η_0^2 against λ/η_0 for $\gamma = 0.00129$ and different values of v and κ; $\backslash\kappa = 0\backslash\kappa = 0.035$.

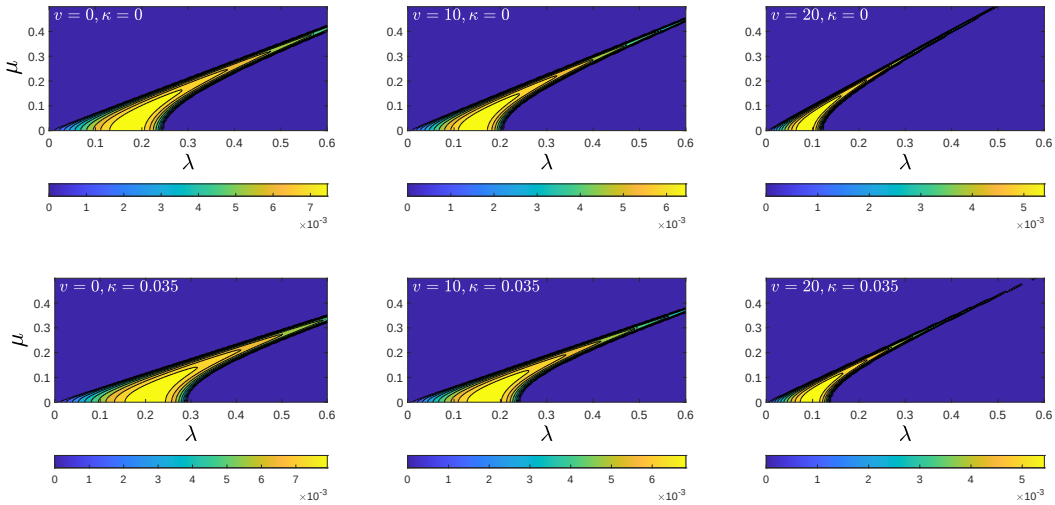

FIGURE 5. Contour plots of $\Omega_i(\lambda, \mu)$ for $\gamma = 0.00129$, $\eta_0 = 0.1$ and different values of v and κ.

4. CONCLUSION

The fourth-order NLEE for deep water CGW including the effect of wind blowing over water is used here to make the stability analysis of uniform wavetrain propagating at the air-water interface. The purpose of the current study is to examine the influence of wind on the BFI. Our analysis is valid if the wind velocity is less than a critical velocity v_c which depends on air-water density ratio and coefficient of surface tension. The key results of the present instability analysis are: (1) Fourth-order effect reduces the GRI. (2) The maximum GRI decreases with the increasing wind

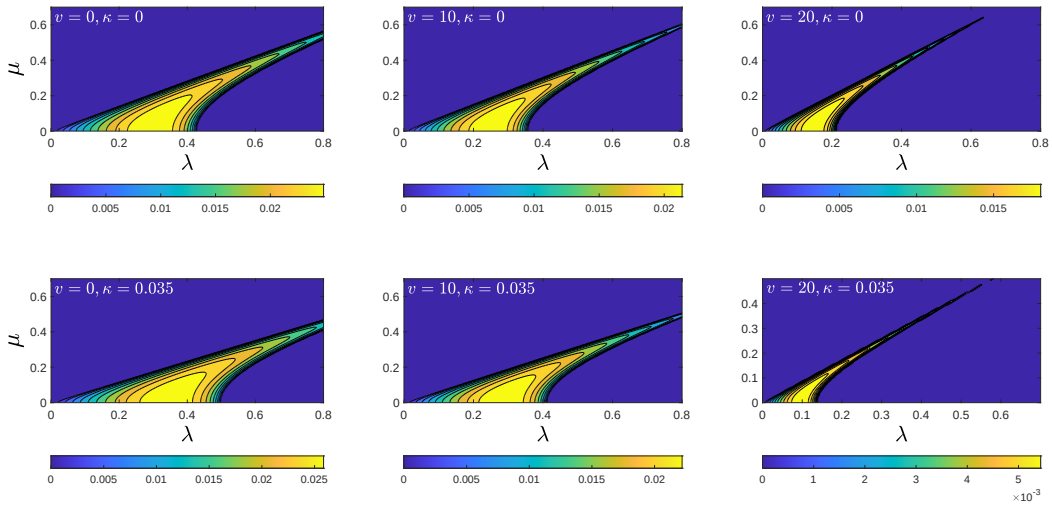

FIGURE 6. Same legend as in figure 5, but $\eta_0 = 0.2$.

velocity. (3) The region of instability reduces with the increase of wind velocity, whereas it increases with the increase of both the wave steepness and surface tension. (4) Effects of wind velocity and surface tension make changes on the contours of frequency separation of fastest growing sideband. It is to be noted that the wind velocity considerably modifies the sideband instability properties.

Appendix : The coefficients appearing in equation (2.1):

$$\delta_1 = -\frac{dc_g}{dk},\ c_g = \left(\frac{d\sigma}{dk}\right)_{k=1},\ \delta_2 = \frac{1-\gamma+3\kappa}{h_\sigma},$$
$$\delta_3 = \frac{2i}{h_\sigma}\left[(1+\gamma)c_g\frac{dc_g}{dk} - \kappa\right],\ \delta_4 = \frac{2i}{h_\sigma}\left[\frac{c_g(1+\gamma)(1-\gamma+3\kappa)}{h_\sigma} + \frac{1-\gamma-3\kappa}{2}\right],$$
$$\Lambda_1 = \frac{\beta_1}{h_\sigma},\ \Lambda_2 = \frac{2}{h_\sigma}\left[\beta_3 - \beta_2 c_g + \frac{2(1+\gamma)c_g\beta_1}{h_\sigma} - 6\kappa\right],$$
$$\Lambda_3 = \frac{2}{h_\sigma}\left[\beta_4 + \frac{(1+\gamma)c_g\beta_1}{h_\sigma}\right],\ \Lambda_4 = \frac{8}{h_\sigma}[\sigma^2 + \gamma(\sigma-v)^2],$$

where

$$\beta_1 = 4\left[\sigma^2 + \gamma(\sigma-v)^2 + \frac{\{\sigma^2-\gamma(\sigma-v)^2\}^2}{1-\gamma-2\kappa} + \frac{3\kappa}{4}\right],$$
$$\beta_2 = 8\left[\frac{\sigma+\gamma(\sigma-v)}{2} + \frac{\{\sigma-\gamma(\sigma-v)\}\{\sigma^2-\gamma(\sigma-v)^2\}}{1-\gamma-2\kappa} - \frac{\{\sigma+\gamma(\sigma-v)\}\{\sigma^2-\gamma(\sigma-v)^2\}^2}{(1-\gamma-2\kappa)^2}\right],$$

$$\beta_3 = -2\Bigg[\sigma^2+\gamma(\sigma-v)^2+\frac{\{4\gamma v(\sigma-v)+(1-\gamma)+12\kappa\}\{\sigma^2-\gamma(\sigma-v)^2\}^2}{(1-\gamma-2\kappa)^2}$$
$$+2\{\sigma^2+\gamma(\sigma-v)(\sigma-2v)\}+\frac{\{\sigma^2-\gamma(\sigma-v)^2\}\{\sigma^2-\gamma(\sigma-v)(\sigma-3v)\}}{1-\gamma-2\kappa}$$
$$+\frac{2\{\sigma^2-\gamma(\sigma-v)(\sigma-2v)\}\{\sigma^2-\gamma(\sigma-v)^2\}}{1-\gamma-2\kappa}\Bigg],$$
$$\beta_4 = -2\left[\sigma^2+\gamma(\sigma-v)^2+\frac{\{\sigma^2-\gamma(\sigma-v)^2\}^2}{1-\gamma-2\kappa}\right],\ h_\sigma = 2[\sigma+\gamma(\sigma-v)].$$

References

[1] C. Brantenberg and I. Brevik, *Higher order water waves in currents of uniform vorticity in the presence of surface tension*, Phys. Scr. **47** (1993), 383–393.

[2] K. B. Dysthe, *Note on a modification to the nonlinear Schrödinger equation for application to deep water waves*, Proc. R. Soc. Lond. **A369** (1979), 105–114.

[3] A. K. Dhar and K. P. Das, *A fourth–order evolution equation for deep water surface gravity waves in the presence of wind blowing over water*, Physics of Fluids A: Fluid Dynamics **2** (1990), 778–783.

[4] S. J. Hogan, *The fourth-order evolution equation for deep-water gravity-capillary waves*, Proc. R. Soc. Lond. **A402** (1985), 359–372.

[5] H. C. Hsu, M. Francius, P. Montalvo and C. Kharif, *Gravity–capillary waves in finite depth on flows of constant vorticity*, Proc. R. Soc. A. **472** (2016), 20160363.

[6] V. M. Hur, *Shallow water models with constant vorticity*, European Journal of Mechanics - B/Fluids **73** (2016), 170–179.

[7] H. C. Hsu, C. Kharif, M. Abid, and Y. Chen, *A nonlinear Schrödinger equation for gravity–capillary water waves on arbitrary depth with constant vorticity. Part 1*, J. Fluid Mech. **854** (2018), 146–163.

[8] P. A. E. M. Janssen, *On fourth order envelope equation for deep water waves*, J. Fluid Mech. **126** (1983), 1–11.

[9] M. S. Longuet-Higgins, *The instabilities of gravity waves of finite amplitude in deep water I. Superharmonics*, Proc. R. Soc. Lond. **A360** (1978), 471–488.

[10] M. S. Longuet-Higgins, *The instabilities of gravity waves of finite amplitude in deep water I. Subharmonics*, Proc. R. Soc. Lond. **A360** (1978), 489–505.

[11] D. P. Majumder and A. K. Dhar, *Stability analysis from fourth order nonlinear evolution equation for two stokes wave trains in deep water in the presence of air flowing over water*, IJAME **4** (2009), 989–1008.

[12] M. Stiassnie, *Note on the modified nonlinear Schrödinger equation for deep water waves*, Wave Motion **6** (1984), 431–433.

Manuscript received 28 December 2023
revised 21 November 2024

S. Halder
Department of Mathematics, Indian Institute of Engineering Science and Technology, Shibpur, Howrah, 711103, West Bengal, India
E-mail address: souravhalder76@gmail.com

A. K. Dhar
Department of Mathematics, Indian Institute of Engineering Science and Technology, Shibpur, Howrah, 711103, West Bengal, India
E-mail address: asoke.dhar@gmail.com